

Long-wavelength collective excitations of charge carriers in high-T_c superconductors

N. Nücker, Ulrich Eckern, J. Fink, P. Müller

Angaben zur Veröffentlichung / Publication details:

Nücker, N., Ulrich Eckern, J. Fink, and P. Müller. 1991. "Long-wavelength collective excitations of charge carriers in high-T_c superconductors." *Physical Review B* 44 (13): 7155–58. <https://doi.org/10.1103/physrevb.44.7155>.

Nutzungsbedingungen / Terms of use:

licgercopyright

Dieses Dokument wird unter folgenden Bedingungen zur Verfügung gestellt: / This document is made available under these conditions:

Deutsches Urheberrecht

Weitere Informationen finden Sie unter: / For more information see:

<https://www.uni-augsburg.de/de/organisation/bibliothek/publizieren-zitieren-archivieren/publiz/>



Long-wavelength collective excitations of charge carriers in high- T_c superconductors

N. Nücker, U. Eckern, and J. Fink

*Kernforschungszentrum Karlsruhe, Institut für Nukleare Festkörperphysik, P.O.B. 3640,
W-7500 Karlsruhe, Federal Republic of Germany*

P. Müller

*Walther-Meissner-Institut für Tieftemperaturforschung, Walther-Meissner-Strasse 8,
W-8046 Garching bei München, Federal Republic of Germany*

(Received 10 April 1991; revised manuscript received 18 July 1991)

The long-wavelength dispersion of the charge-carrier plasmon in $\text{Bi}_2\text{Sr}_2\text{CaCu}_2\text{O}_8$ for wave vectors parallel to the CuO_2 planes has been investigated by transmission-electron energy-loss spectroscopy. For the [100] and the [110] directions the size of the quadratic plasmon dispersion differs by a factor of about 2. This strong in-plane anisotropy can be explained by a calculation in the framework of the random-phase approximation using a simple tight-binding ansatz for the CuO band having a quadratic Fermi surface. However, a different Fermi surface at a lower-energy scale cannot be excluded.

Since the discovery of the high- T_c superconductors,¹ the nature of the normal state is the central issue for the understanding of the mechanism for high- T_c superconductivity. The reason for the complex electronic structure of these compounds are the strong correlation effects on the Cu sites, which may lead to a breakdown of the usual single-particle model. Currently, it seems that only after investigating many different aspects of the normal state at different characteristic energy scales will a clear picture of the electronic structure of cuprate superconductors emerge. For the understanding of the electronic structure of nearly-free-electron metals the experimental and theoretical investigation of collective excitations and their wave vector dependence was of fundamental importance. Therefore, the dispersion of the charge-carrier plasmons in doped cuprates also is of great interest. Previously the dispersion of the 1-eV charge-carrier plasmon in $\text{Bi}_2\text{Sr}_2\text{CaCu}_2\text{O}_8$ has been studied by two groups.^{2,3} Although there was qualitative agreement between these measurements, a significant difference in dispersion coefficients appeared, which was explained in Ref. 3 by small variations in the stoichiometry of the samples.

Moreover, we mention a long-standing puzzle for cuprate superconductors;⁴ the plasmon frequencies ω_p , as derived from an evaluation of reflectivity data within a simple Drude model, are almost independent of the dopant concentration x (for not too small x). This would be expected for a nearly half-filled antibonding CuO band where ω_p^2 should be proportional to $1-x$. Consistent with this expectation are also angular resolved photoemission measurements which indicate a large Fermi-surface typical of a half-filled CuO_2 band.⁵ In contrast, however, Hall-effect measurements⁶ show that the charge-carrier concentration is proportional to x corresponding to a small Fermi surface.

In this paper we present extended investigations of the long-wavelength dispersion of the charge-carrier plasmon in $\text{Bi}_2\text{Sr}_2\text{CaCu}_2\text{O}_8$ by electron-energy-loss spectroscopy (EELS). For wave-vectors parallel to the CuO_2 planes a strong anisotropy between the [100] and the [110] direc-

tion is detected. The anisotropy can be explained in terms of a quadratic Fermi surface, thus pointing to the dominance of the electrons which are nested along the Γ - X , Γ - Y directions.^{7,8}

Single crystalline $\text{Bi}_2\text{Sr}_2\text{CaCu}_2\text{O}_8$ was grown from a stoichiometric mixture of the oxides pressed to a pellet. The sample was kept for 10 h at 980°C and then cooled down by 2.2°C/h to 830°C. Subsequently the single crystals formed were annealed in Ar for 10 h at 720°C. Investigation of the superconducting transition by a superconducting quantum interference device at 20 mOe field gave 87.1 and 85.7 K for the 90% and 10% transition temperatures, respectively, and a Meissner fraction of 44%. Thin films about 100-nm thick were peeled off the single crystal using a tape. The tape glue was subsequently dissolved in CHCl_3 , and the thin film was floated on a 0.1-mm-diam hole of a copper disk.

The transmission EELS measurements were performed at room temperature using a 170 keV spectrometer described elsewhere.⁹ The energy- and momentum-transfer resolutions were chosen to be 0.13 eV and 0.05 \AA^{-1} , respectively. The single crystalline films were oriented in the spectrometer by angular scanning of Bragg reflections. In the [100] direction, besides a strong 200 reflection, a low intensity 100 reflection was observed. In the [010] direction, the b direction, strong superstructure reflections with a period of 0.23 \AA^{-1} , i.e., $\sim 0.2b_0$, were detected. This clearly showed that the films were twin free single crystals. Due to increased multiple scattering for momentum transfers near Bragg reflections of the superstructure, precise measurements of the plasmon dispersion in the b direction were restricted to momentum transfers apart from these values.

Figure 1 shows the loss function $\text{Im}(-1/\epsilon)$ for low-energy excitations as measured for momentum transfer $q=0.1$ and 0.3 \AA^{-1} . The measurements were contaminated at energies below 0.5 eV by the direct or quasielastic peak due to the finite resolution in energy and momentum transfer. The curves therefore were extrapolated to zero energy (dashed lines). While for small momentum

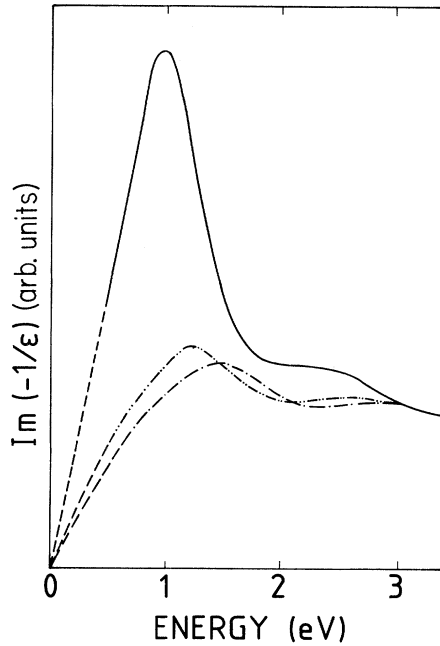


FIG. 1. Loss functions $\text{Im}[-1/\epsilon(q, \omega)]$ for $\text{Bi}_2\text{Sr}_2\text{CaCu}_2\text{O}_8$. Solid line: momentum transfer $q=0.1 \text{ \AA}^{-1}$, $\mathbf{q} \parallel [100]$ or $[110]$; dashed-dotted line: $q=0.3 \text{ \AA}^{-1}$, $\mathbf{q} \parallel [100]$; dashed-double-dotted line: $q=0.3 \text{ \AA}^{-1}$, $\mathbf{q} \parallel [110]$. Dashed lines: extrapolations to zero. All curves are normalized between 3 and 4 eV.

transfers $q \leq 0.1 \text{ \AA}^{-1}$ no energy dependence versus the direction of the momentum transfer in the a, b plane could be detected, a significant energy shift of the plasmon peak for $q=0.3 \text{ \AA}^{-1}$ is apparent in Fig. 1. Also, there is a strong increase of the width with increasing q . The orientation dependence of the plasmon energy for momentum transfers $q=0.3 \text{ \AA}^{-1}$ in the a, b plane is shown in Fig. 2 in more detail. The energy of the plasmon peak has a minimum for momentum-transfer parallel to the $[110]$ direction (angle $\Phi=45^\circ$) and maxima for \mathbf{q} parallel to the $[010]$ and $[100]$ directions ($\Phi=0^\circ$ and 90° , respectively).

Figure 3 gives peak positions of the plasmon as measured for momentum transfers ranging from 0.05 to 0.4 \AA^{-1} in the $[100]$ and $[110]$ crystallographic directions. Due to strong damping of the plasmon and low cross sections for higher-momentum transfers, data for momentum transfers above $q=0.4 \text{ \AA}^{-1}$ were not included. The plasmon dispersion can be described in both directions by $E_p(q) = E_p(0) + (\hbar^2/m)\alpha_{hk0}q^2$ with $E_p(0)=1 \text{ eV}$, $\alpha_{100}=0.63$, and $\alpha_{110}=0.35$. The dispersion coefficients derived from previous measurements (Ref. 2: $\alpha=0.60$; Ref. 3: $\alpha=0.40$) are in the range between α_{100} and α_{110} . Since the anisotropy of the dispersion coefficient was not noticed in these investigations, the discrepancy between the results of the two groups finds now a natural explanation.

An anisotropy of the plasmon dispersion (even in cubic crystals) has been previously reported in nearly-free-electron metals and in semiconductors.^{10,11} It has been explained within the random phase approximation including band structure using one electron energies and wave

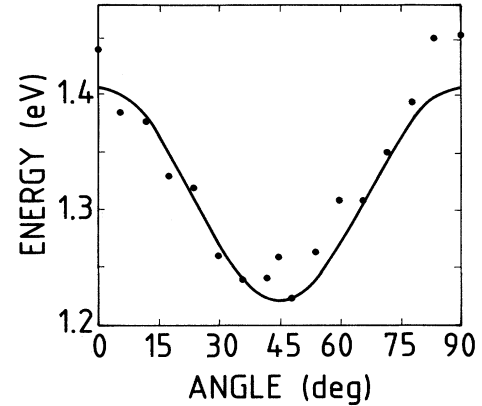


FIG. 2. Variation of the energy of the charge-carrier plasmon in $\text{Bi}_2\text{Sr}_2\text{CaCu}_2\text{O}_8$ for momentum transfer $q=0.3 \text{ \AA}^{-1}$ as a function of the rotation angle Φ of the direction of the momentum transfer around the $[001]$ axis. $\Phi=0^\circ$: $\mathbf{q} \parallel [010]$; $\Phi=45^\circ$: $\mathbf{q} \parallel [110]$; $\Phi=90^\circ$: $\mathbf{q} \parallel [100]$. Solid line: theoretical estimate as given in Eq. (7), with $\hbar\omega_p=1 \text{ eV}$, $t=1.5 \text{ eV}$, and $a=3.8 \text{ \AA}$.

functions determined by a pseudopotential approximation.¹² Therefore, as a first attempt, it is reasonable to perform a similar calculation for $\text{Bi}_2\text{Sr}_2\text{CaCu}_2\text{O}_8$. The situation in this system is more complicated since according to band-structure calculations^{7,8} and angular-resolved photoemission spectroscopy results⁵ there should be two Fermi surfaces, one related to the CuO_2 planes and one to electron pockets due to BiO planes. Since these electron pockets contribute only a small amount of charge carriers and since their Fermi surfaces are almost circular we neglect them in the following calculation. We also have neglected contributions to the plasmon anisotropy caused by anisotropic oscillators above the plasmon frequency which may be apparent when regarding in Fig. 1 the intensities at $E \sim 2.8 \text{ eV}$ for $q=0.3 \text{ \AA}^{-1}$. However, we be-

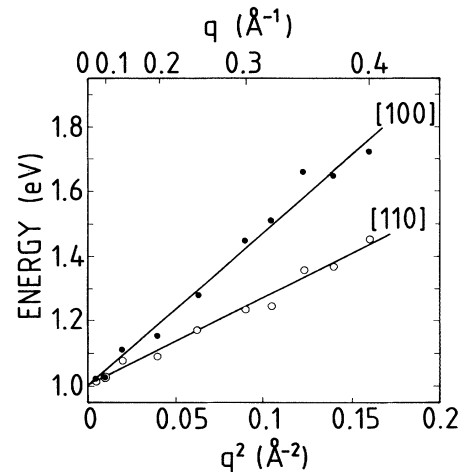


FIG. 3. Dispersion of the charge-carrier plasmon in $\text{Bi}_2\text{Sr}_2\text{CaCu}_2\text{O}_8$ for momentum transfer $\mathbf{q} \parallel [100]$ (solid circles) and $\mathbf{q} \parallel [110]$ (open circles). Solid lines: $\alpha=0.63$ and 0.35 , respectively.

lieve that this intensity difference is caused by double scattering.

As usual, the plasmon dispersion is obtained from the condition

$$\text{Re}\epsilon(\mathbf{q}, \omega) = 0; \quad \epsilon(\mathbf{q}, \omega) = 1 + \frac{4\pi}{q^2} \chi(\mathbf{q}, \omega). \quad (1)$$

For the density response function we take the Lindhard-

$$\chi(\mathbf{q}, \omega) = -\frac{2e^2}{(\hbar\omega)^2} \left[\langle (\mathbf{q} \cdot \mathbf{v})^2 \rangle_{\text{FS}} + \frac{\langle (\mathbf{q} \cdot \mathbf{v})^4 \rangle_{\text{FS}}}{(\hbar\omega)^2} + \frac{1}{12} \left\langle (\mathbf{q} \cdot \mathbf{v}) \left[\mathbf{q} \cdot \frac{\partial}{\partial \mathbf{k}} \right]^2 (\mathbf{q} \cdot \mathbf{v}) \right\rangle_{\text{FS}} \right], \quad (3)$$

where $\mathbf{v} = \partial E_k / \partial \mathbf{k}$, and the (not normalized) Fermi-surface average is defined by

$$\langle (\dots) \rangle_{\text{FS}} = \int \frac{d^3k}{(2\pi)^3} (-f')(\dots) \quad (4)$$

and $-f' \approx \delta(E_k - E_F)$. Note that in (3), the first two terms on the right-hand side also follow from the Boltzmann-equation approach. The last term, for the approximate band structure to be discussed below, leads only to small corrections to the plasmon dispersion, and will be neglected in the following.¹³

Guided by the nesting feature of the CuO_2 bands along the Γ -X, Γ -Y directions, we assume an extremely simplified band structure. Consider the Cu 3*d* and O 2*p* orbitals, whose overlap is given by the transfer integral *t* (taken to be equal in the *x* and *y* directions), and assume in addition $E_p \approx E_d$. Then the upper (antibonding) band close to half filling is given by¹⁴

$$E_{\mathbf{k}} \approx -\frac{1}{2} t (\cos k_x a + \cos k_y b), \quad (5)$$

where $a (=b)$ denotes the O-O distance. For half filling, the Fermi surface is thus the square given by $\cos k_x a = -\cos k_y b$.

Given the band structure (5), the Fermi-surface averages in (3) are easily computed with the result $8\pi e^2 \times \langle (\mathbf{q} \cdot \mathbf{v})^2 \rangle_{\text{FS}} = (\hbar\omega_p)^2 q^2$, where the plasma frequency is given by the standard expression $\omega_p^2 = 4\pi e^2 n/m^*$; for half filling $n = (a^2 c)^{-1}$ and $m^* = (\pi\hbar)^2 / 2ta^2$. With¹⁵ $q_x = q \cos(\Phi + \pi/4)$, $q_y = q \sin(\Phi + \pi/4)$, we find (half filling)

$$\langle (\mathbf{q} \cdot \mathbf{v})^4 \rangle_{\text{FS}} = \frac{nt^3(aq)^4}{6\pi^2} \left(\frac{3}{2} + \frac{1}{2} \cos 4\Phi \right) \quad (6)$$

and hence the plasmon dispersion is given by

$$(\hbar\omega_q)^2 = (\hbar\omega_p)^2 + \frac{1}{6} (ta)^2 q^2 \left(\frac{3}{2} + \frac{1}{2} \cos 4\Phi \right). \quad (7)$$

Note that $(3 + \cos 4\Phi)/2$ varies between two and one for Φ between 0 and $\pi/4$; this anisotropy follows immediately by considering $\langle (\mathbf{q} \cdot \mathbf{v})^4 \rangle_{\text{FS}}$ for a square Fermi surface, by noting that on the Fermi surface we have $v_x = \pm v_y$.

Inserting standard parameters: $a \approx 3.8$ Å, $c \approx 30.9/4$ Å ≈ 7.7 Å (which takes care of the fact that there are four CuO_2 planes per unit cell), and $t \sim 1.5$ eV, we find $\hbar\omega_p \sim 2.67$ eV in reasonable agreement with the experimental result, if we take into account the reduction of the

Ehrenreich-Cohen expression

$$\chi(\mathbf{q}, \omega) = -4e^2 \int \frac{d^3k}{(2\pi)^3} f(E_k) \frac{\Delta E}{(\hbar\omega + i0)^2 - (\Delta E)^2}, \quad (2)$$

where the matrix elements are replaced by their free-electron values, and where $\Delta E = E_{k+q} - E_k$. Equation (2) is evaluated in the long-wavelength limit; hence expanding with respect to ΔE and integrating by parts, we arrive at

plasma frequency by the background dielectric constant² ($\epsilon_\infty \approx 4.5$). In addition, the dispersion coefficient α is given by $\alpha \approx 0.71$ and 0.35 , for $\Phi = 0$ and $\pi/4$, respectively, which also is in good agreement with the experiment. (Here we used the experimental value $\hbar\omega_p \sim 1$ eV. For the above parameters, we have $n \approx 9 \times 10^{21}/\text{cm}^2$ and $m^*/m \approx 1.7$.) Note also that the size of the dispersion is given by the slope of the band at the Fermi surface, i.e., $\sim (ta)^2$.

In conclusion, though we do not wish to stress the numerical agreement between theory and experiment too much, the present results indicate that the charge-carrier plasmon and its dispersion in $\text{Bi}_2\text{Sr}_2\text{CaCu}_2\text{O}_8$ are very well described by the simple model of a half-filled band. In particular, the anisotropy by about a factor of 2 is a direct consequence of the Fermi surface being (close to) a square, provided that these contributions dominate (strong dispersion along the nesting directions).

Comparing with the results of band-structure calculations,^{7,8} these show indeed a Fermi surface with large parts strongly nested along the Γ -X, Γ -Y directions. However, one would also expect contributions from the remaining parts of the Fermi surface, and it is thus presently not clear whether the anisotropy by about two will survive if the realistic band structure is used. We remark that, for the Tl compound, a simple band structure has been suggested,¹⁶ including the next-nearest-neighbor coupling. However, for this band structure, for which the Fermi surface almost seems to be a "square" rotated by 45° , we find that the plasmon dispersion should be almost isotropic, and in fact slightly smaller ($\sim 20\%$) along the Γ -X, Γ -Y directions. This clearly differs from our results for the Bi compound.

Considering the damping of the plasmon (see Fig. 1), the width of the peak for $q = 0.1$ Å⁻¹ is ~ 1 eV, and increases strongly with increasing momentum transfer. In order of magnitude, this value (for small *q*) is in agreement with theoretical estimates based on marginal¹⁷ or nested¹⁸ Fermi-liquid theories. Additional measurements at 40 K confirm, within the accuracy of our results, that the width is temperature independent, as to be expected since $\hbar\omega_p \gg kT$. The strong increase of the width with increasing *q*, presumably related to increasing interband transitions, also requires further studies.

Altogether, it is surprising that the anisotropy of the plasmon dispersion is so well reproduced by our simple an-

satz, in which correlation effects are not taken into account. In particular, we mention the current and lively discussion whether or not the normal state of the high- T_c superconductors behaves like a Fermi liquid and whether local-density approximation (LDA) band-structure calculations are meaningful. We cannot decide this question in general; however, though some open questions remain, our results indicate that for energies ~ 1 eV and for sufficient doping, a LDA-type calculation can give a good description of the electronic properties. The situation is different for smaller dopant concentrations, where a transition from a metallic into an insulating state is observed, due to strong correlation effects, and no plasmon is found in optical⁴ and EELS¹⁹ measurements.

In particular, more detailed evaluation of optical data^{4,20-22} show that the reflectivity data of the cuprates cannot be explained by a simple Drude model.²³ Rather, the data could be fitted in terms of a generalized Drude model having a frequency and temperature-dependent scattering rate or by a two-component model with a Drude term and an additional Lorentz oscillator in the mid-infrared (IR) region. The oscillator strength of the two components is concentration dependent. At small concentration, the Drude term is almost zero and the Lorentz term is larger. In the overdoped systems, the mid-IR absorption is small and the Drude term is large.

At a dopant concentration where T_c is at maximum, the two components have the same order of magnitude.²¹ There are numerous explanations for the mid-IR absorption.⁴

Since the oscillator energy of the Lorentz term is considerably smaller than the plasma frequency ω_p , both the Drude term and the Lorentz term contribute to the 1 eV plasmon. This situation is similar to heavily doped Si where bound electrons with a binding energy of ~ 3 eV lead to a "free-electron" plasmon at 17 eV. Therefore, we suggest that in the cuprate superconductors the plasmon at 1 eV is composed of free electrons and bound electrons. The present results show that at an excitation energy of 1 eV the sum of the two components behaves as predicted by a simple band structure, i.e., a large Fermi surface is detected. However, at lower energies where only the free electrons have to be taken into account (bound electrons are no more excited) the picture may be quite different. Possibly a small Fermi surface would emerge (at least for small x) in agreement with the Hall data.⁶ We emphasize that we cannot exclude a non-Fermi-liquid behavior at low energies. Unfortunately, the present energy resolution in our spectrometer does not allow to study the free-electron plasmon which may be detectable at intermediate dopant concentrations at low temperatures, i.e., for small relaxation rates.

¹J. G. Bednorz and K. A. Müller, Z. Phys. B **64**, 189 (1986).

²N. Nücker, H. Romberg, S. Nakai, B. Scheerer, J. Fink, Y. F. Yan, and Z. X. Zhao, Phys. Rev. B **39**, 12379 (1989).

³Y.-Y. Wang, G. Feng, and A. L. Ritter, Phys. Rev. B **42**, 420 (1990).

⁴See, e.g., Th. Timusk and D. B. Tanner, in *Physical Properties of High Temperature Superconductors I*, edited by D. M. Ginsberg (World Scientific, Singapore, 1989), p. 339.

⁵C. G. Olson, R. Liu, D. W. Lynch, R. S. List, A. J. Arko, B. W. Veal, Y. C. Chang, P. Z. Jiang, and A. P. Paulikas, Phys. Rev. B **42**, 381 (1990); J. C. Campuzano, G. Jennings, M. Faiz, L. Beaulaigue, B. W. Veal, J. Z. Liu, A. P. Paulikas, K. Vandervoort, H. Claus, R. S. List, A. J. Arko, and R. J. Bartlett, Phys. Rev. Lett. **64**, 2308 (1990); G. Mante, R. Claessen, T. Buslaps, S. Harm, R. Mancke, M. Skibowski, and J. Fink, Z. Phys. B **80**, 181 (1990).

⁶See, e.g., P. B. Allen, Z. Fisk, and A. Migliori, in *Physical Properties of High Temperature Superconductors I* (Ref. 4), p. 213.

⁷H. Krakauer and W. E. Pickett, Phys. Rev. Lett. **60**, 1665 (1988); see also W. E. Pickett, Rev. Mod. Phys. **61**, 433 (1989).

⁸S. Massidda, J. Yu, and A. J. Freeman, Physica C **152**, 251 (1988).

⁹J. Fink, Adv. Electron. Electron Phys. **75**, 121 (1989).

¹⁰H. Raether, *Excitation of Plasmons and Interband Transitions by Electrons* (Springer-Verlag, Berlin, 1980).

¹¹J. Sprösser-Prou, A. vom Felde, and J. Fink, Phys. Rev. B **40**, 5799 (1989).

¹²K. Sturm, Adv. Phys. **31**, 1 (1982).

¹³Strictly speaking, the condition that the last term on the right-hand side of (3) is negligible, is given by $\omega_p^2 \ll t^2$. Note also the numerical factor of $\frac{1}{12}$.

¹⁴J. Friedel, J. Phys. Condens. Matter **1**, 7757 (1989).

¹⁵We emphasize that $\Phi=0$ corresponds to the [100], or equivalently the [010], direction of the orthorhombic unit cell (see Ref. 8).

¹⁶J. Yu, S. Massidda, and A. J. Freeman, Physica C **152**, 273 (1988).

¹⁷C. M. Varma, P. B. Littlewood, S. Schmitt-Rink, E. Abrahams, and A. E. Ruckenstein, Phys. Rev. Lett. **63**, 1996 (1989).

¹⁸J. Ruvalds and A. Virosztek, Phys. Rev. B **43**, 5498 (1991).

¹⁹H. Romberg, N. Nücker, J. Fink, Th. Wolf, X. X. Xi, B. Koch, H. P. Geserich, M. Dürer, W. Assmus, and B. Gegenheimer, Z. Phys. B **78**, 367 (1990).

²⁰G. A. Thomas, J. Orenstein, D. H. Rapkine, M. Capizzi, A. J. Millis, R. N. Bhatt, L.F. Schneemeyer, and J. V. Waszczak, Phys. Rev. Lett. **61**, 1313 (1988).

²¹S. Uchida, T. Ido, H. Takagi, T. Arima, Y. Tokura, and S. Tajima, Phys. Rev. B **43**, 7942 (1991).

²²I. Terasaki, T. Nakahashi, S. Takebayashi, A. Maeda, and K. Uchinokura, Physica C **165**, 152 (1990).

²³Based on the small differences of the measured dispersion coefficient (Refs. 2 and 3), it was argued in Ref. 3 that $n \sim m^*$, and thus n/m^* is independent of x , although $n \sim x$. This interpretation is not supported by our present detailed results.